

Beam Calorimeter Technologies

R. Dollan, Ch. Grah, E. Kouznetsova, W. Lange, W. Lohmann, A. Stahl

DESY, Zeuthen, Germany

K. Afanaciev, V. Drugakov

NCPHEP, Minsk, Belarus

Two different technologies are considered for the Beam Calorimeters of the ILC detector. Simulation studies of the performance have been done for a diamond-tungsten sandwich calorimeter and for a homogeneous heavy element crystal calorimeter with optical fiber readout. Studies of the stability and the linearity of a polycrystalline diamond were done for the diamond-tungsten option. For the heavy crystal option the light yield reduction due to the wavelength shifting fiber readout was studied.

1. INTRODUCTION

The Beam Calorimeter (BeamCal) will be positioned just adjacent to the beampipe in front of the final focus quadrupoles covering very low angles (4-28) mrad. One of the purposes of the BeamCal is to serve a fast beam diagnostics detecting e^+e^- pairs originated from the beamstrahlung photons conversion. The calorimeter provides a good hermiticity of the whole detector and allows to measure high energy electrons down to the very low angles. The calorimeter also shields the inner part of the detector from backscattered beamstrahlung remnants and synchrotron radiation.

The beamstrahlung remnants create huge energy deposition in the BeamCal. The total energy deposited in the calorimeter is about ~ 20 TeV per bunch crossing for nominal TESLA beam parameters and detector design. The deposited energy varies significantly with radius and azimuthal angle, providing areas of very high occupancy. The integrated radiation dose of up to 10 Gy/year is expected for these areas [1] requiring radiation hardness to the BeamCal sensitive material.

Measurements of high energetic electrons or photons on top of the beamstrahlung remnants require a high transversal granularity and a small Moliere radius of the calorimeter.

One of the considered technologies for the BeamCal is a diamond-tungsten sandwich calorimeter. Polycrystalline Chemical Vapour Deposition (pCVD) diamonds have been shown to be sufficiently radiation hard [2]. A sketch of a possible calorimeter structure is shown in Figure 1.

Another technology considered for the BeamCal design is a heavy element homogeneous calorimeter where scintillator segments are read out with optical fibers. A longitudinal segment of the crystal calorimeter is shown in Figure 2. Every piece of the segment is optically isolated from the neighbors and read out with a wavelength shifting fiber. The fiber is routed to the back of the calorimeter through optically isolated grooves in the adjacent rear parts. As a possible material for the calorimeter lead tungstenate (PbWO_4) is considered in the simulations.

2. SIMULATION OF THE CALORIMETER PERFORMANCE

The beamstrahlung is simulated using the Monte Carlo program Guinea Pig [3]. Single high energy electrons are simulated with energies between 50 and 250 GeV using the GEANT3 [4] based detector simulation package BRAHMS [5].

The reconstruction procedure was tuned to provide less than 1% of fake events. The fake rate was estimated by applying the reconstruction algorithm to a pure background events.



Figure 1: The structure of a half barrel of the sandwich calorimeter. Between the tungsten disks diamond sensors are interspersed.

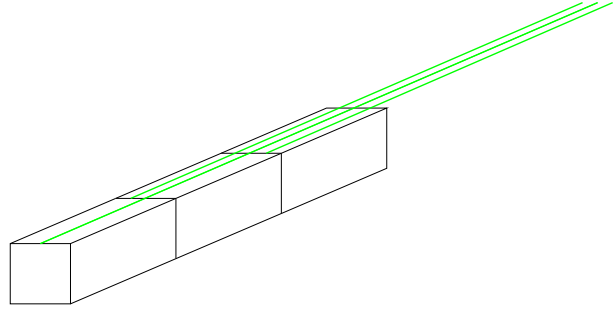


Figure 2: Scintillator pieces forming a longitudinal segment of the crystal calorimeter. Each piece is connected to an optical fiber routed to the back of the calorimeter.

2.1. Diamond-Tungsten Calorimeter

The simulated calorimeter consists of 30 tungsten disks alternating with diamond sensor layers. The thickness of the tungsten disks is chosen to be 3.5 mm (one radiation length), the diamond layers are 0.5 mm thick. Every diamond layer is segmented into pads. The number of pads in a ring increases with the radius keeping pad dimensions of about half a Moliere radius (5 mm).

Figure 3 shows a detection efficiency as a function of the radius for electrons of different energies. The efficiencies are obtained at azimuthal angle around $\phi = 90^\circ$ where the background level is high. Figure 4 shows a map of cells where the detection efficiency is less than 90%. Electron energies between 50 and 250 GeV are considered.

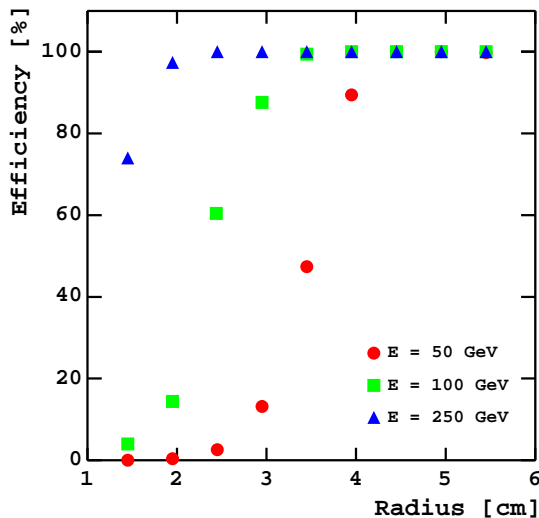


Figure 3: The efficiency to detect electrons of 50, 100 and 250 GeV in the high background region ($\phi \approx 90^\circ$) of the BeamCal as a function of the radius of the calorimeter.

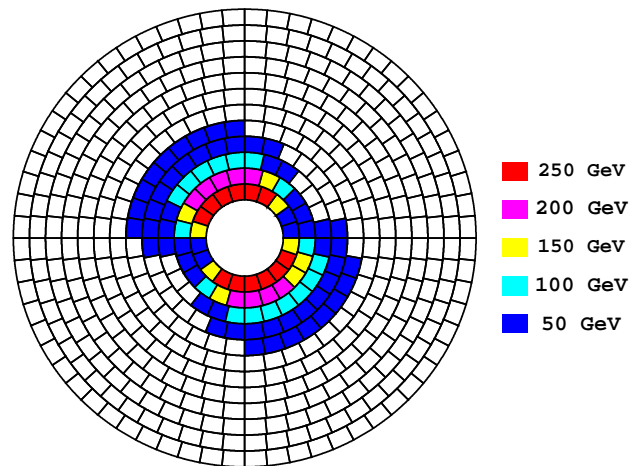


Figure 4: A map of low-efficiency regions. The cells where the detection efficiency for a high energetic electron is less than 90% are marked with colors corresponding to the electron energy.

2.2. Heavy Scintillator Calorimeter

The study of a lead tungstate calorimeter performance are done the same way. The transverse segmentation is chosen to be of about half a Moliere radius (~ 1 cm). Every segment was divided longitudinally into tree pieces as it is shown in Figure 2. The length of the pieces is 3, 9 and 8 radiation lengths starting with a front side of the calorimeter. To investigate the influence of the fibers and wrapping material on the calorimeter performance, an ideal homogeneous calorimeters has been studied as well as a realistic one. Figure 5 shows a cross-section of a frontal calorimeter segment with wrapping and an attached fiber as it was implemented for the realistic simulation.

Figure 3 shows the efficiency to detect a 100 GeV electron in the low background region at azimuthal angle around $\phi = 0^\circ$ as a function of the radius. The deterioration of the performance due to the wrapping and fiber material is clearly seen.

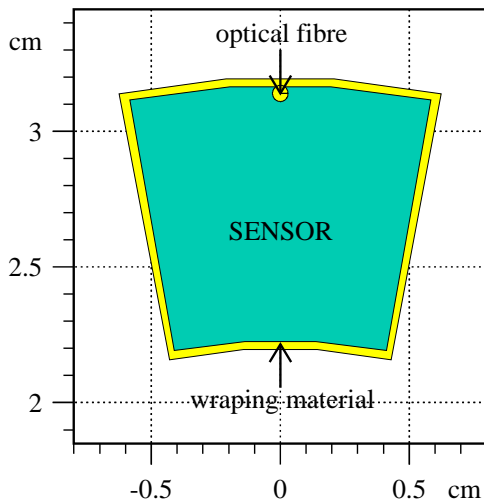


Figure 5: A cross-section of a frontal calorimeter segment with wrapping and wavelength shifting fiber.

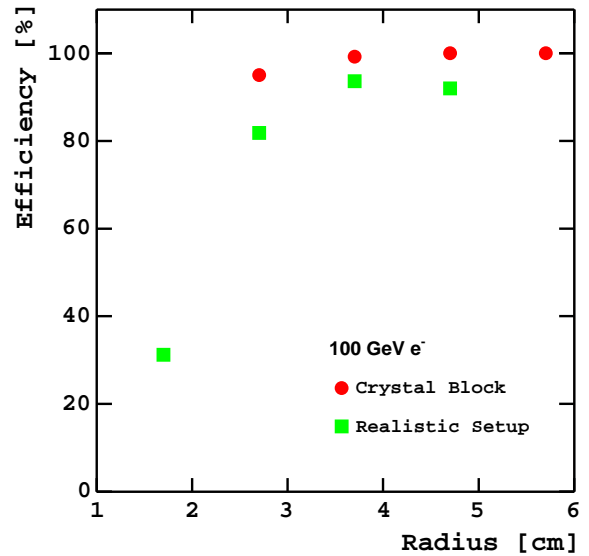


Figure 6: The detection efficiency for 100 GeV electrons in the low background region as a function of the radius. The results for the ideal (circles) and realistic calorimeter with fibers and wrapping material (squares) are shown.

3. SENSOR STUDIES FOR DIAMOND-TUNGSTEN OPTION

Polycrystalline CVD diamond samples produces in Fraunhofer Institute (Freiburg, Germany), have been tested for the diamond-tungsten option of the BeamCal. The samples have 10×10 mm² area with a two-layer Ti/Au metalization and thickness between 200 and 500 μ m.

Measurements of the charge collection efficiency under low irradiation doses have been done in order to check stability of the signal. A diamond response to irradiation with a ^{90}Sr beta-source was monitored up to absorbed dose of at least 20 Gy. The voltage applied during the irradiation corresponded to the electric field of 1 V/ μ m.

Top plot of Figure 7 shows the mean values of the ^{90}Sr spectrum obtained with diamond samples as a function of the absorbed dose. The charge collection efficiency stabilized after the dose of about 15 Gy. Stability of current in the high voltage circuit during is shown on bottom plot of Figure 7.

Figure 8 shows results for another diamond sample. The current increased with the absorbed dose and depended on the dose rate. Stabilization of the current and charge collection efficiency has been obtained at about 20 Gy.

The linearity of diamond response has been tested with a hadron beam of about 4 GeV at the CERN PS. Beam spills of about 10 ns duration with variable intensity (up to 10^7 mips per a spill) produced an integrated signal in a diamond sample. A scintillator with two photomultipliers attached was used as a trigger and a reference for the linearity measurements. An example of the measurement results is shown in Figure 9.

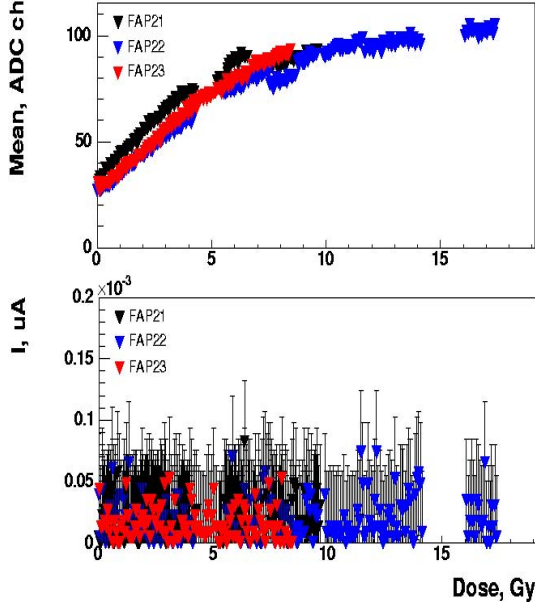


Figure 7: The mean values of the ^{90}Sr spectrum (top) and current in the high voltage circuit (bottom) obtained for three samples as function of the absorbed dose.

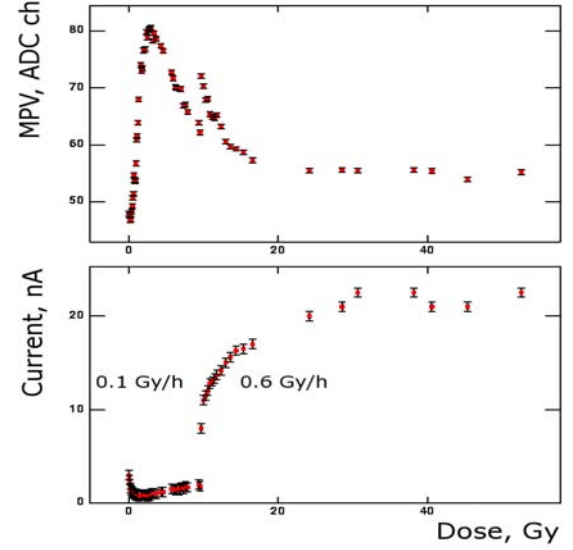


Figure 8: The mean values of the ^{90}Sr spectrum (top) and current in the high voltage circuit (bottom) as function of the absorbed dose. The dose accumulation rate was changed at about 10 Gy.

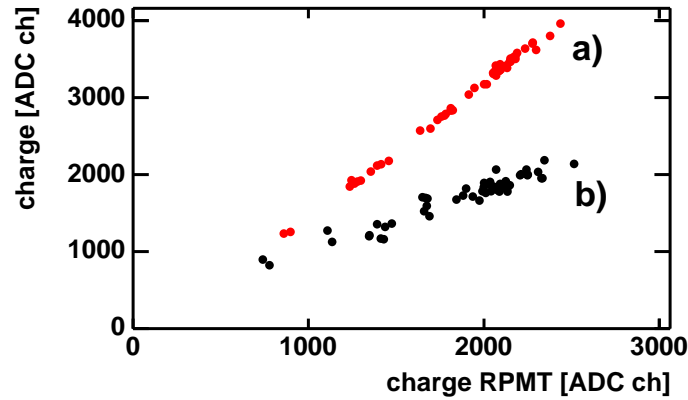


Figure 9: The signal from a diamond (a) and one of the photomultipliers (b) as a function of the signal from the second photomultiplier.

4. STUDIES OF FIBER READOUT FOR CRYSTAL OPTION

4.1. Light Yield Reduction and Crosstalk Measurements

Measurements of light yield reduction due to the fiber readout have been done in order to test the feasibility of the concept. The measurements are done using plastic scintillator (Bicron BC-408 [6]) and lead glass as the test samples. These two materials have different light production mechanism: in the plastic scintillator light is produced due to scintillation, in lead glass via the Čerenkov effect. Light produced in a crystal under tests due to traversing cosmic muons is read out by a photomultiplier tube coupled to the scintillator directly (Setup "a" in Figure 10, left) or via a Bicron BCF-19A wavelength shifting fiber (Setup "b" in Figure 10, left). An example of the obtained spectra are shown in Figure 10, right. The fiber readout reduced the light yield to $(14 \pm 4)\%$ for plastic scintillator and to $(16 \pm 7)\%$ for lead glass.

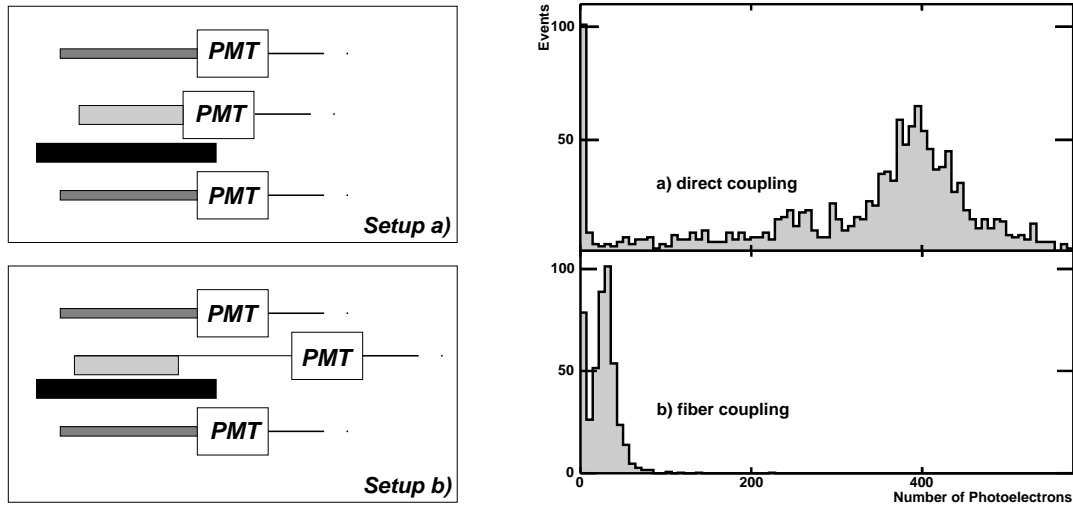


Figure 10: Setup for light yield measurements (left). The scintillator under the test is positioned between triggering scintillators and read out directly (Setup "a") or via a wavelength shifting fiber (Setup "b"). The signal spectra obtained from relativistic cosmic muons for Setup "a" and Setup "b" (Right).

To estimate the crosstalk for the considered readout, measurements with a plastic scintillator segmented into three pieces were done. Every segment had one readout fiber attached and wrapping for optical insulation. The fibers were routed to one side as it is shown in Figure 2 and are optically isolated from the neighboring segments.

All three fibers were read out with photomultipliers. Setup "b" shown in Figure 10 was rearranged such to produce a trigger signal only for muons traversing the first segment, where all three fibers were routed through. The signals from the other two fibers were monitored. The crosstalk level was estimated to be less than 1%.

4.2. Simulation Studies of Light Yield Reduction

The transport of optical photons generated in a crystal was simulated using GEANT4 [7]. Scintillation and Čerenkov radiation as well as a set of optical processes including the wavelength shifting mechanism were taken into account. The wavelength shifting process is available since version 6.0 of GEANT4. The simulation is done for the plastic scintillator and lead glass crystals of the same geometry as in the measurements of light yield reduction. A cross-section of the crystal is shown in Figure 11. The wavelength shifting fiber and its connection to the crystal were thoroughly implemented including the fiber material, fiber cladding and optical glue. The wavelength shifting process was based on the absorption and emission spectra of BCF-19A fibers provided by Bicron. For the simulation no optimization of the material surfaces and the material boundary conditions were done.

A light yield reduction to (9.3-9.8)% for the plastic scintillator and (8.3-12.0)% for the lead glass has been obtained from the simulation, that is in a good agreement with the results of measurement.

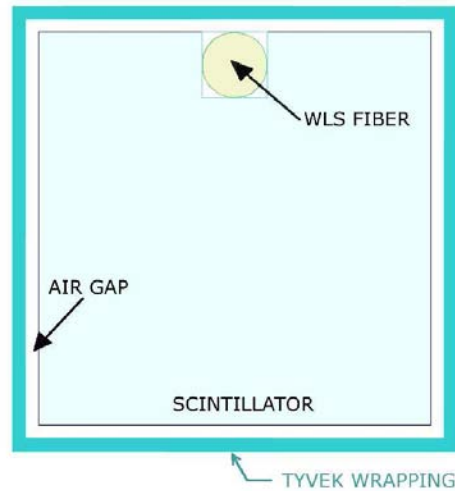


Figure 11: A cross-section of the scintillator considered in the simulation. The scintillator has a rectangular slot with a glued wavelength shifting fiber.

5. CONCLUSION

The simulation studies of the BeamCal performance showed the considered technologies to be feasible. The efficiency to detect electrons with energy of about 100 GeV and higher is almost 100% for most of the calorimeter area.

The ongoing studies of diamond samples for the diamond-tungsten options are done in contact with the diamond manufacturer (Fraunhofer Institute). The goal of the work is to prepare a calorimeter prototype with reliable diamond sensors for further studies in a test-beam.

The fiber readout for the heavy crystal calorimeter is shown to be feasible. The GEANT4 simulation of the light transportation is shown to be in a good agreement with the measurement results. That allows to include it to the realistic simulation of the heavy crystal BeamCal.

References

- [1] H. Abramowicz et al., "Instrumentation of the Very Forward Region of a Linear Collider Detector", IEEE trans. on Nuclear Science, 5, 6, 2004
- [2] T. Behnke et al., "Electromagnetic Radiation Hardness of Diamond Detectors", arXiv:hep-ex/0108038 v1, 2001
- [3] D. Schulte, Ph.D Thesis, Hamburg 1996, <http://www-sldnt.slac.stanford.edu/nlc/beamdeliveryhome.htm>
- [4] http://wwwasdoc.web.cern.ch/wwwasdoc/geant_html3/geantall.html
- [5] T. Behnke et al., http://www-zeuthen.desy.de/linear_collider
- [6] Saint-Gobain CRYSTALS and DETECTORS, <http://www.bicron.com>
- [7] <http://wwwasd.web.cern.ch/wwwasd/geant4/geant4.html>